



Preconcentration of heavy metal ions on magnetic multi-walled carbon nanotubes using magnetic solid-phase extraction and determination in vegetable samples by electrothermal atomic absorption spectrometry: Box–Behnken design

Sara Khodadadi¹ · Elahe Konozi¹ · Ali Niazi¹ · Ali Ezabadi¹

Received: 27 January 2022 / Accepted: 15 June 2022 / Published online: 22 July 2022
© Institute of Chemistry, Slovak Academy of Sciences 2022

Abstract

In this study, a simple, rapid, and efficient analytical method was proposed for the preconcentration and determination of trace amounts of cadmium and chromium in vegetable samples using magnetic solid-phase extraction (MSPE) coupled with electrothermal atomic absorption spectrometry (ETAAS) detection. Magnetic multi-walled carbon nanotubes (MWCNTs) as an effective adsorbent were synthesized and characterization was performed using scanning electron microscope, transmission electron microscopy, Fourier-transform infrared spectroscopy, X-ray diffraction, and vibrating-sample magnetometer. The experimental parameters were optimized using Box–Behnken design and maximum absorbance of Cd (II) and Cr (VI) was obtained at pH=5, adsorbent dosage of 0.02 and 0.12 g, ligand concentration of 4 $\mu\text{g L}^{-1}$, and extraction time of 22.5 min. The accuracy was assessed through proper recoveries in the range of 58.63–99.03% and 62.86–89.69% for Cd (II) and Cr (VI), respectively. In addition, precision was evaluated with a relative standard deviation (RSD) below 2.8% for both analytes. Linearity was in the range of 5–100 $\mu\text{g L}^{-1}$ for both metal ions. The limit of detection and limit of quantification values were found below 0.3 $\mu\text{g L}^{-1}$ and 0.3 $\mu\text{g L}^{-1}$ using the ETAAS technique, respectively. The magnetic MWCNTs as a promising and low-cost adsorbent can be used in MSPE along with AAS approaches for the extraction and determination of heavy metal ions in several vegetable samples.

Keywords Magnetic solid-phase extraction · Multi-walled carbon nanotubes · Electrothermal atomic absorption spectrometry · Heavy metals · Vegetable samples · Box–Behnken design

Introduction

Heavy metals can enter into the environment such as surface and groundwater, soil, and crop plants owing to human activities. Anthropogenic activities, including agriculture, steel and iron industry, mining, smelting processes, chemical manufacturing, domestic activities, tannery effluent sludge, compost waste, as well as fly ash are the main origins related to the heavy metals (Manzoor et al. 2018). Chromium (Cr), cadmium (Cd), copper (Cu), zinc (Zn), lead (Pb), mercury (Hg), manganese (Mn), and nickel (Ni) are known in the category of these contaminants (Arora 2019). Cadmium is

tremendously hazardous to humans, which leads to serious problems in various organs such as lungs, kidneys, and liver. Its accumulation in tissues and organs can remain for many years. It is possible to excrete a small amount of cadmium from the body (Öztürk Er et al. 2018). Hexavalent chromium (VI) is very soluble and mobile, which damages the liver, respiratory organs, kidneys, and skin, causing different diseases like renal tubular necrosis, lung cancer, dermatitis, and perforation of the nasal septum (Zhong et al. 2016).

One of the major routes in which heavy metals enter the body is vegetables. The amount of heavy metal accumulation in vegetables depends on the agricultural soil and environmental conditions (Altunay and Katin 2020). Vegetables possess an essential role in the human diet owing to the presence of useful and necessary minerals and nutrients in their structure. Edible and non-edible parts of vegetables can uptake heavy metals higher than the permissible limit

✉ Elahe Konozi
konozelahe@gmail.com

¹ Department of Chemistry, Central Tehran Branch, Islamic Azad University, Tehran, Iran

(Kumar et al. 2019). The maximum level of cadmium in vegetables and leafy vegetables has been reported 0.05 and 0.2 mg kg⁻¹ wet weight, respectively (Altunay and Elik 2021; Commission Regulation 2011). Also, the allowable concentration of chromium in vegetable samples has been stated 2.3 mg kg⁻¹ (Ashraf et al. 2021; Ahrham and Gholap 2021). The growth of plants in soils contaminated with heavy metals and the consumption of these plants cause them to enter the food chain. Finally, their accumulation in living organisms is dangerous to human and animal health (Odobasic et al. 2017).

Numerous methods such as electrothermal atomic absorption spectrometry (ETAAS) (Oliveira Lopes and Rocha Chellini 2020), high-resolution continuum source graphite furnace atomic absorption spectrometry (HR-CS GF-AAS) (Pozzatti et al. 2017), inductively coupled plasma optical emission spectrometry (ICP-OES) (Feist and Mikula 2014), voltammetry (Palisoc et al. 2018; Locatelli and Melucci 2013), and flame atomic absorption spectrometry (FAAS) (Daşbaşı et al. 2015) have been used to determine heavy metals in different matrices.

Among these procedures, minimal sample preparation volume and the utilization of direct analysis without or minimum sample preparation are the advantages of the ETAAS approach. Also, the ETAAS possesses good sensitivity, low detection limit, and the possibility of automation. However, the lack of adequate sensitivity for low concentrations of metal ions and complex matrices is its drawback. Therefore, the preconcentration step is essential before determination (Arpa and Arıdaşir 2019; Ling et al. 2021).

Several techniques, including coprecipitation (Saçmacı and Kartal 2010; Ipeaiyeda and Ayoade 2017), membrane filtration (Divrikli et al. 2007), dispersive liquid–liquid microextraction (Sorouraddin et al. 2020), and cloud point extraction (Kamel et al. 2019; Karadaş 2015), have been reported for the preconcentration of metal ions. Time-consuming, excessive consumption of organic solvents, unfavorable enrichment factors, as well as secondary wastes are disadvantages of these methods (Roushani et al. 2017).

One of the most remarkable used procedures for the separation and preconcentration of metal ions is magnetic solid-phase extraction (MSPE) due to its simplicity, high yield, low-cost, and high selectivity (Ibarra et al. 2015). The basis of this method is the usage of magnetic adsorbent for the adsorption and desorption of analyte. The magnetic material maintains the target compound. Then, the separation of the magnetic particle (containing the analyte) from the sample solution is performed using an external magnetic field (Hagarov 2020). Low stability of magnetic nanoparticles (NPs) such as Fe₃O₄ and γ -Fe₂O₃ in solution, mainly in acidic solution, is known as their limitations, which results

in the decomposition of materials and the loss of magnetic properties (Yilmaz and Soylak 2020). To overcome this problem, the modification with other materials such as carbon nanotubes (CNTs) is necessary. They have received a lot of attention due to their physical features and many extensive applications. Based on their constituent layers, CNTs are divided into single-walled (SWCNTs) and multi-walled (MWCNTs). Unlike SWCNTs, MWCNTs possess excellent properties like large surface area, prominent structural characteristics, as well as good thermal and mechanical stability (Zhaoa et al. 2021; Pashai Gatabi et al. 2016). Also, their affinity to target compounds can be controlled based on the surface functionalization via chemical or physical techniques (Barbosa et al. 2020).

The magnetic MWCNTs have been showed super operational stability and the maintenance great adsorption and magnetic features even after several cycles in the adsorption and desorption process (Chen et al. 2012).

The dithiocarbamate derivative ligands can be used along with an adsorbent for the adsorption of heavy metal ions. Dithiocarbamates have nitrogen and sulfur atoms in different hybridized states, which cause a powerful ability to form chelate toward metal ions. These ligands have a great ability to adsorb heavy metals because of electron sharing between nitrogen, sulfur atoms, as well as metal ions (Abu-El-Halawa and Zabin 2017).

In this study, synthesized magnetic MWCNTs as an efficient and simple adsorbent along with 8-dithiocarbamate ligand were used in the MSPE method for the preconcentration of Cd and Cr ions in various vegetable samples. The fabricated magnetic MWCNTs were characterized using a scanning electron microscope (SEM), transmission electron microscopy (TEM), Fourier-transform infrared spectroscopy (FTIR), X-ray diffraction (XRD), and vibrating-sample magnetometer (VSM). In addition, ETAAS were used to determine the values of the mentioned ions. The effective parameters in the extraction process, including pH, adsorbent dosage, ligand concentration, and time, were optimized through response surface methodology (RSM) based on Box–Behnken design (BBD). To the best of our knowledge, there are no reports for the extraction of Cd (II) and Cr (VI) ions from the vegetable samples using magnetic MWCNTs.

Experimental

Materials

The standard solutions of 1000 mg L⁻¹ cadmium and chromium were provided from Chem-Lab (Belgium). Also, ferric

chloride hexahydrate ($\text{FeCl}_3 \cdot 6\text{H}_2\text{O}$), ferrous chloride tetrahydrate ($\text{FeCl}_2 \cdot 4\text{H}_2\text{O}$), carbon nanotube (99%), methanol, ethanol, acetonitrile, and dimethylformamide (DMF) were purchased from Merck (German). Dried vegetable samples, including basil, pennyroyal, parsley, and mint, were procured from local supermarkets (Tehran, Iran).

Apparatus

The determination of cadmium and chromium concentrations was performed using PerkinElmer ETAAS (PinAAcle 900 T, USA). The operating parameters for the ETAAS analysis of mentioned heavy metals are given in Table 1. FE-SEM (KYKY Technology, China) was used to determine the surface morphology of the adsorbent. The functional groups of synthesized adsorbent were studied by FTIR (JACSO-FTIR-410, Japan) with a KBr pellet. The crystallographic structure related to the adsorbent was investigated using XRD (X'pert-MPD, Netherland). VSM (LBKFB model, Meghnatis Daghigh, Kavir Co., Iran) was utilized to study the magnetic property of Fe_3O_4 -MWCNTs. TOPwave microwave (Analytik Jena, Germany) was utilized to digest the dried vegetable samples. Vacuum oven (BINDER, Germany) and ultrasonic bath (BANDELIN, 35 kHz, Germany) were also used for drying the samples and homogenizing the solutions, respectively. A pH meter (Sartorius, USA) was used to adjust the pH value of the solutions.

Synthesis of Fe_3O_4 NPs

Five g of $\text{FeCl}_2 \cdot 4\text{H}_2\text{O}$ and 12.5 g of $\text{FeCl}_3 \cdot 6\text{H}_2\text{O}$ were dissolved into 65 mL deionized water. Then, 2 mL of concentrated HCl was added into the solution. Six hundred mL of NaOH solution (1.5 M) was poured into the round-bottom flask and under vigorous stirring at 70 °C was added drop wise into the previous solution for 1 h. The obtained black magnetic NPs were washed three times with deionized water and dried in an oven at a temperature of 60 °C for 24 h (Lü et al. 2016).

Table 1 Operating parameters for the ETAAS analysis of heavy metals

Elements	Wave-length (nm)	Detection limit ($\mu\text{g/g}$)	Slit width (nm)	Lamp current (mA)	Gas flow (L/min)
Cd	228.8	0.00005	0.7	8	1
Cr	357.9	0.00002	0.7	10	1

Synthesis of magnetic MWCNTs

The CNTs and Fe_3O_4 NPs were combined with each other with a ratio of 1:1 (w/w). In this procedure, dispersion of CNTs (2 g) in DMF (50 mL) was accomplished by sonication. Afterward, 2 g of Fe_3O_4 NPs was added, which were previously dispersed in 50 mL of DMF. Then, sonication was performed for 15 min, as well as for the facile separation, 300 mL distilled water was added. The collection of magnetic CNTs from the mixture was carried out using a nylon membrane ($0.45 \mu\text{m} \times 47 \text{mm}$). Eventually, washing with water and drying (at 90 °C for 24 h) were conducted. In order to prevent oxidation, the magnetic CNTs were kept under a vacuum atmosphere (Mohamad Nasir et al. 2019).

Real sample preparation

0.4 g of each dried vegetable sample was accurately weighed. Then, the samples were separately digested with 6 mL of concentrated HNO_3 at 170 °C in microwave digestion. The solutions were evaporated using a hot plate at a temperature of 200 °C and mixed with 1 mL of H_2O_2 . Afterward, 100 mL of deionized water was added to the digested samples.

MSPE procedure

Samples containing 25 mL of chromium and cadmium with the concentration of $1 \mu\text{g L}^{-1}$ were added to the $4 \mu\text{g L}^{-1}$ of 8-dithiocarbamate as a ligand. Then, 0.02 g and 0.12 g of the magnetic CNTs was added to the chromium and cadmium solution, respectively with pH = 5. The mixture was stirred at 360 rpm for 22.5 min with constant speed at room temperature. Afterward, an external magnet was used to separate the adsorbent from the aqueous phase. Two mL of methanol–nitric acid (0.5mol L^{-1}) and acetonitrile–nitric acid (0.5mol L^{-1}) were added to the adsorbent and stirred for 22.5 min. The clear phase contains chromium and cadmium ions, which were measured by ETAAS.

Design of experiments (DOE)

One-factor-at-a-time (OFAT) approach is used to optimize the experimental parameters. In this method, one variable is changed and the other variables are constant. Its disadvantages include high laborious, high cost, and time-consuming. In order to overcome these drawbacks, response surface methodology (RSM) has been used. It is a statistical method that the interaction among the factors is evaluated and the

Table 2 The range of pH, adsorbent dosage, ligand concentration, and extraction time in the BBD

Factor	Variables	Lower limit	Upper limit
A	pH	3	7
B	Adsorbent dosage (g)	0.02	0.12
C	Ligand concentration ($\mu\text{g L}^{-1}$)	0.5	4
D	Extraction time (min)	5	40

optimum conditions are selected. Box–Behnken design (BBD) is known as one such RSM (Parmar et al. 2020).

The optimization of the effective variables, as well as the interaction between them, can be facilitated with the least number of experiments using BBD. It is an inexpensive alternative to central composite design (CCD) due to its fewer factor levels, as well as the lack of extremely high and low levels (Parmar et al. 2020; Polat and Sayan 2019).

In this study, Design-Expert 10.0 was used to implement the BBD method. The effect of experimental parameters, including pH, adsorbent dosage, ligand concentration, and time of extraction was assessed to achieve the optimal levels and the interactions between the factors. The ranges of the variables (lower limit and higher limit) related to each factor were specified (Table 2).

The number of runs in the BBD is obtained by Eq. (1).

$$N = 2K(K - 1) + C_0 \quad (1)$$

In this equation, the number of variables and the repeat number of runs at a center point are indicated by K and C_0 , respectively (Rais et al. 2021). In this study, 36 runs with 12 replications were performed.

The quadratic response model was considered as the best model, which can be described via Eq. (2).

$$Y = \beta_0 + \sum \beta_i X_i + \sum \beta_{ii} X_{ii}^2 + \sum \beta_{ij} X_i X_j + \varepsilon \quad (2)$$

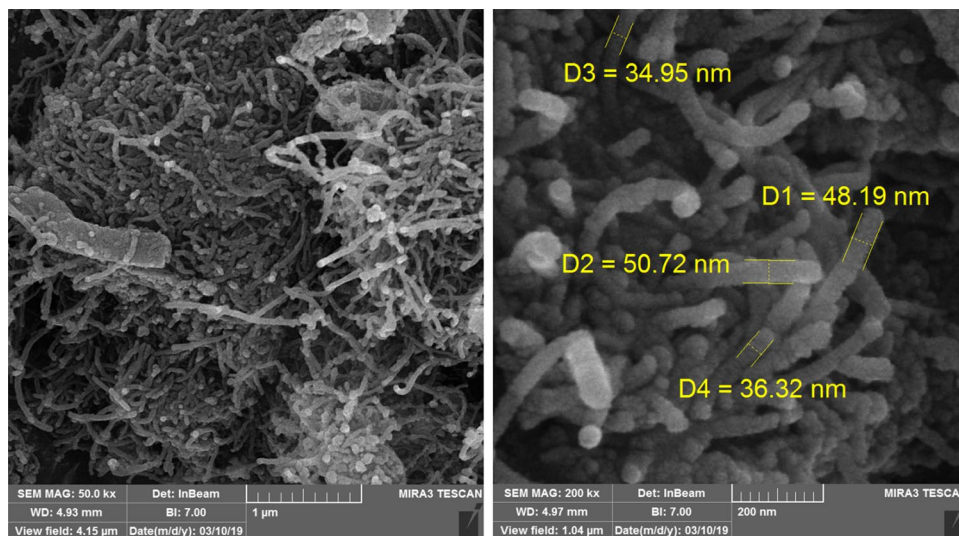
Herein, β_i and β_{ii} denote the linear effect of factor X_i and the square effect of factor X_{ii} , respectively. β_{ij} is linear by the linear effect of the factors X_i and X_j . The unknown constant error vector is represented by ε (Rais et al. 2021).

Results and discussion

Characterization

SEM analysis

Figure 1 exhibits the SEM image of magnetic MWCNTs. As shown, the MWCNTs are similar to the thin strands that a large number of spherical particles are distributed on their

Fig. 1 SEM image of magnetic MWCNTs

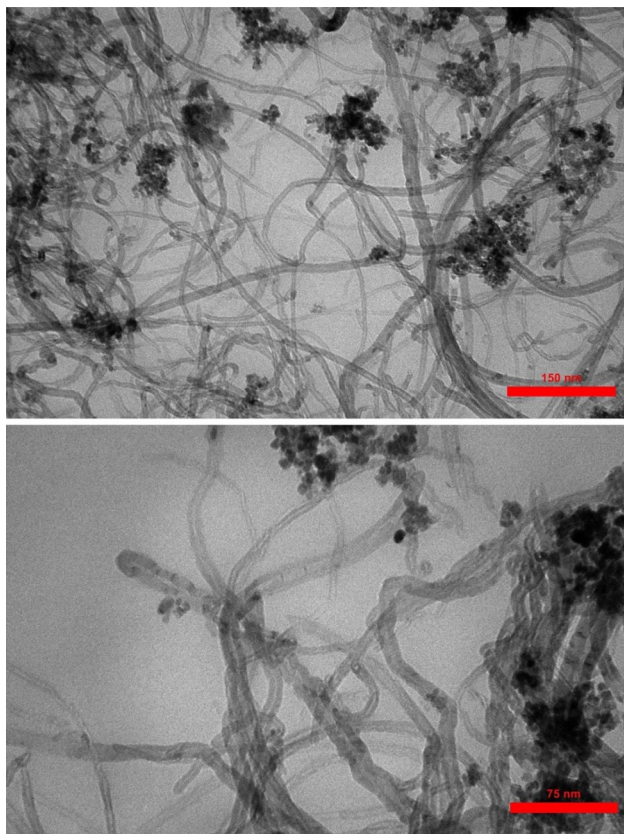
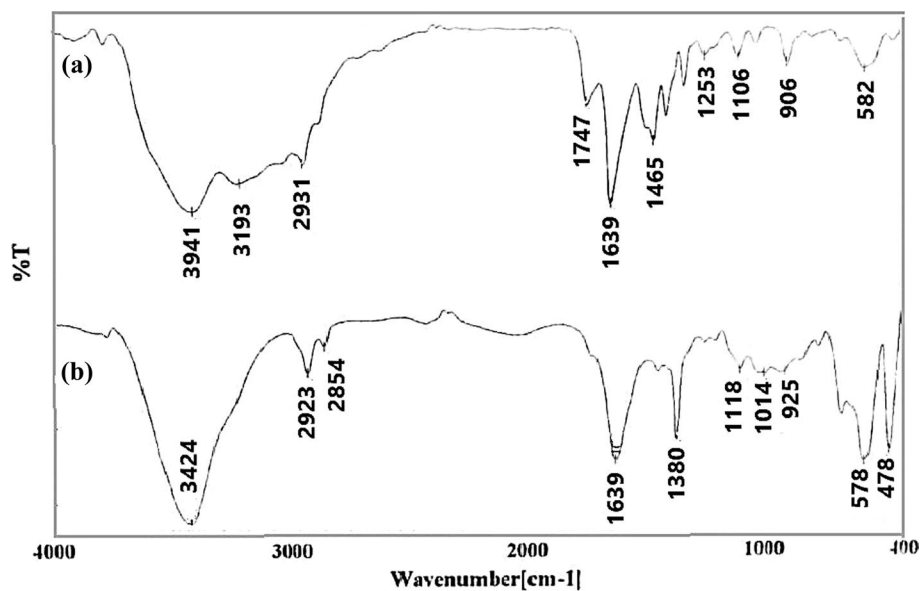


Fig. 2 TEM image of magnetic MWCNTs

surface. The interaction between the carboxyl functional groups and the Fe_3O_4 NPs leads to this linkage.

Fig. 3 FTIR spectra of **a** MWCNTs and **b** magnetic MWCNTs



TEM analysis

The spherical Fe_3O_4 particles are located on the tubular surface of MWCNTs without obvious aggregation (Fig. 2). Complexes containing metal ions and carboxylic acid can be formed owing to numerous number of coordinating functional groups of carboxylic acid (Sadegh et al. 2014). The average size of nanocomposite is 7.75 nm.

FTIR analysis

As shown in Fig. 3a and b, the absorption peaks at 3941 and 3424 cm^{-1} are related to the O–H stretching vibration. The peaks at 2931 and 2923 cm^{-1} are attributed to the stretching or bending modes of $-\text{CH}_2$. The peak appearing at 1747 cm^{-1} corresponded to the stretch mode of carboxylic groups (Wang et al. 2021; Soni et al. 2020). The band located at 1465 cm^{-1} can be related to the O–H bending mode of the COOH group (Pashai Gatabi et al. 2016). The band at 1639 cm^{-1} represents the C=O stretching of the COOH group. The observed peak at 1380 cm^{-1} is assigned to the C–OH stretching. The existence of peaks at 1106 and 1118 cm^{-1} is due to the stretching modes of C–O (Soni et al. 2020). The characteristic peak at 578 cm^{-1} belongs to the Fe–O bending vibration (Lu et al. 2017).

XRD analysis

The XRD pattern of magnetic MWCNTs is shown in Fig. 4. The diffraction peaks at $2\theta = 26.27^\circ$ and 43.56° are dedicated

Fig. 4 XRD pattern of magnetic MWCNTs

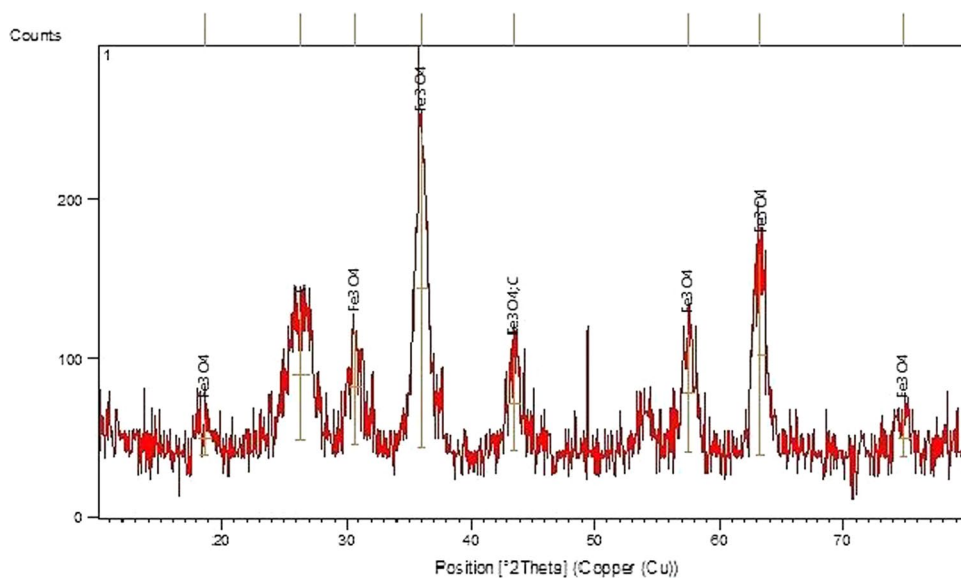
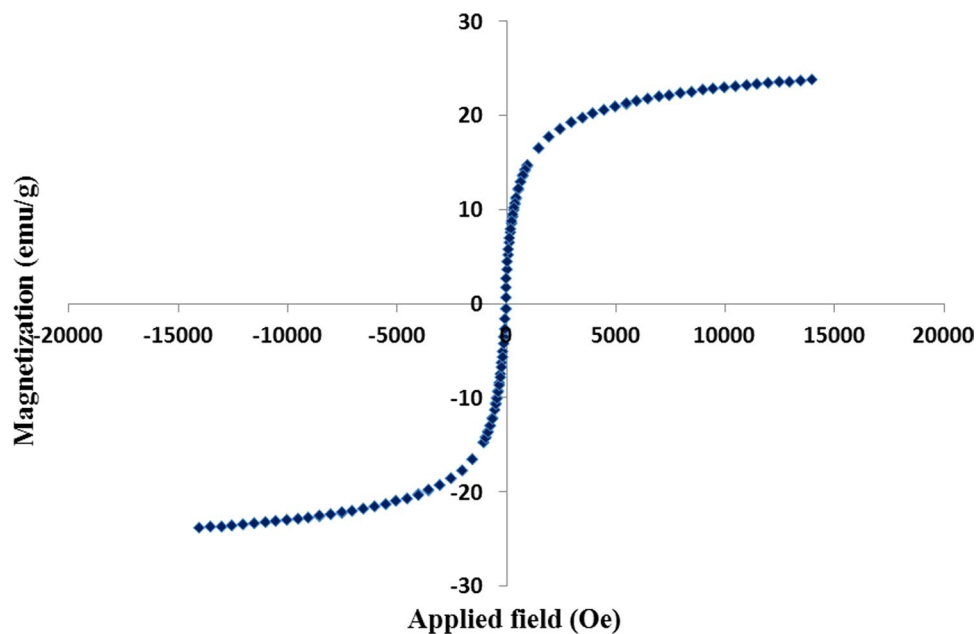


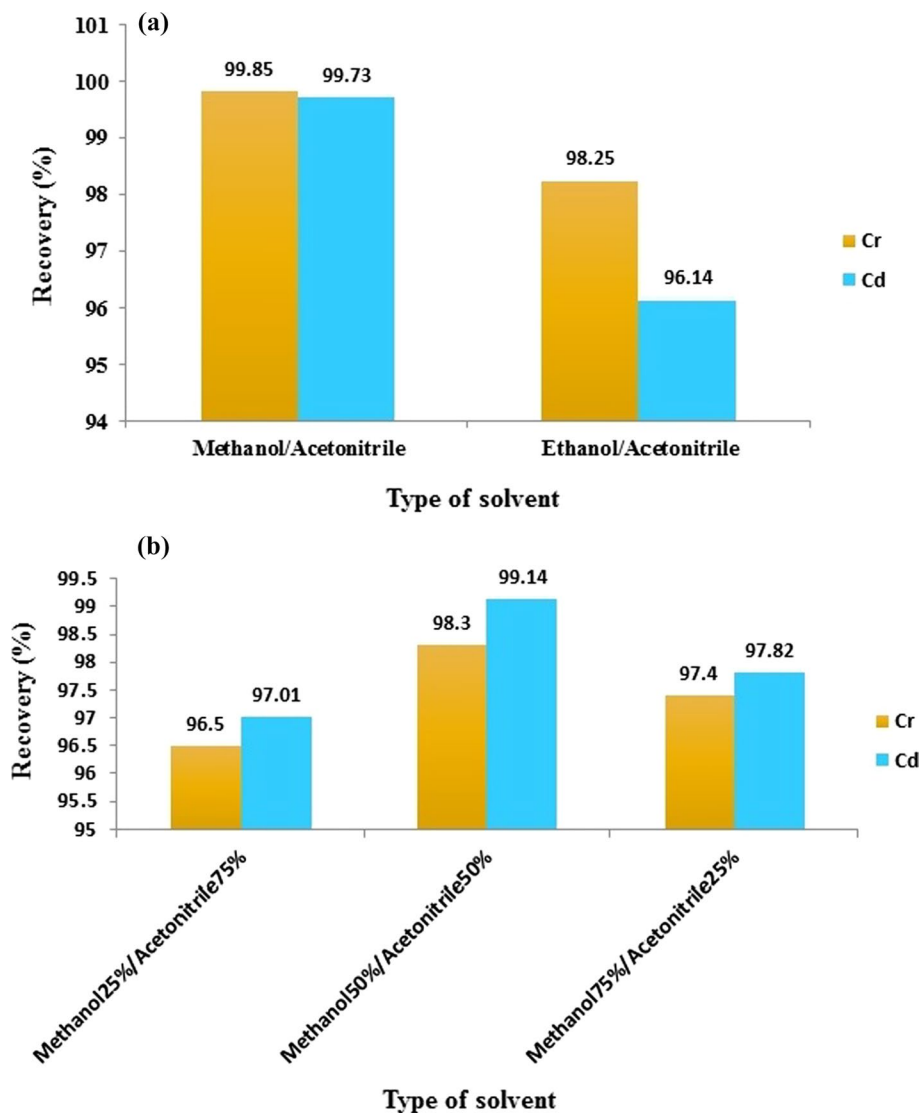
Fig. 5 VSM spectrum of magnetic MWCNTs



to (002) and (100) planes, which represent the hexagonal graphite structure. The main peaks are characterized at $2\theta = 18.66^\circ$, 30.69° , 35.97° , 57.45° , and 62.89° , which assigned to the (111) (220), (311), (511), and (440) crystal

planes, respectively. This pattern is in accordance with the inverse spinel crystalline structure of maghemite (JCPDS file, No. 39–1346) (Pashai Gatabi et al. 2016; Sadeq et al. 2014).

Fig. 6 The effect of **a** different solvents **b** different ratios of methanol/acetonitrile on extraction recovery of Cd (II) and Cr (VI)



VSM analysis

The magnetic intensity of MWCNTs is shown in Fig. 5. The saturation magnetization (σ_s) value of MWCNTs is 23.81 emu g^{-1} . According to the articles, the magnetic property of the Fe_3O_4 -MWCNTs is less than the bare Fe_3O_4 NPs, which is due to the coating Fe_3O_4 NPs with the MWCNTs.

Selecting the best solvent

The solvent type has a significant effect on the yield (Recovery %) (Onyebuchi and Kavaz 2020). In order to

preconcentration of Cd (II) and Cr (VI) ions, two types of solvents, including methanol/acetonitrile (50:50 v/v) and ethanol/acetonitrile (50:50 v/v), were used. Between these solvents, methanol/acetonitrile with a recovery percentage of 99.85 was selected as the best solvent (Fig. 6a). Afterward, different ratios of methanol/acetonitrile (25:75 v/v, 75:25 v/v, 50:50 v/v) were examined. The maximum recovery (98%) was related to the methanol/acetonitrile (50:50 v/v) (Fig. 6b).

One of the main parameters for evaluating the MSPE performance is the preconcentration factor (PF), which is calculated using Eq. (1).

Table 3 Results of BBD and interaction between factors

Run	pH	Adsorbent dosage (g)	Ligand concentration ($\mu\text{g L}^{-1}$)	Extraction time (min)	Abs (Cd)	Abs (Cr)
1	5	0.07	2.25	22.5	0.8488	0.0615
2	5	0.07	2.25	22.5	0.8561	0.0685
3	5	0.07	0.5	5	0.6561	0.0402
4	5	0.07	4	5	0.6833	0.0493
5	3	0.02	2.25	22.5	0.6058	0.0505
6	7	0.12	2.25	22.5	0.8098	0.0575
7	5	0.07	2.25	22.5	0.8541	0.0645
8	5	0.07	0.5	40	0.7894	0.0547
9	5	0.07	4	40	0.9417	0.0717
10	7	0.02	2.25	22.5	0.9281	0.0202
11	5	0.07	2.25	22.5	0.8204	0.0608
12	3	0.12	2.25	22.5	0.7678	0.0705
13	5	0.02	4	22.5	0.9647	0.0229
14	5	0.12	0.5	22.5	0.8804	0.0364
15	3	0.07	2.25	40	0.7014	0.0789
16	5	0.07	2.25	22.5	0.8883	0.0685
17	3	0.07	2.25	5	0.5087	0.0585
18	5	0.07	2.25	22.5	0.8352	0.0656
19	5	0.02	0.5	22.5	0.8054	0.0485
20	7	0.07	2.25	40	0.9011	0.0528
21	5	0.12	4	22.5	0.8855	0.0968
22	5	0.07	2.25	22.5	0.8777	0.0668
23	7	0.07	2.25	5	0.6848	0.0409
24	5	0.07	2.25	22.5	0.8876	0.0689
25	5	0.02	2.25	40	0.8825	0.0495
26	5	0.12	2.25	40	0.9540	0.0897
27	7	0.07	0.5	22.5	0.8963	0.0587
28	5	0.12	2.25	5	0.6754	0.0617
29	5	0.07	2.25	22.5	0.8325	0.0784
30	5	0.07	2.25	22.5	0.8955	0.0804
31	3	0.07	0.5	22.5	0.5242	0.0725
32	5	0.02	2.25	5	0.7845	0.0378
33	5	0.07	2.25	22.5	0.8845	0.0846
34	3	0.07	4	22.5	0.7845	0.0896
35	5	0.07	2.25	22.5	0.8478	0.0746
36	7	0.07	4	22.5	0.7725	0.0687

$$PF = \frac{C_r}{C_f} \quad (3)$$

where C_r and C_s denote the analyte concentration in the elution phase and the initial concentration of the analyte in the sample solution, respectively (Khodadadi et al. 2021). In this study, the preconcentration factor was found to be 100.

Box–Behnken design

According to the results of Table 3, experiments were accomplished and the obtained results are the absorbance of Cd and Cr ions. The absorbance was in the range of 0.5087–0.9647 and 0.0202 to 0.0897 for the Cd and Cr,

respectively. The maximum absorbance of Cd (0.9647) was related to the pH=5, adsorbent dosage of 0.02 g, ligand concentration of $4 \mu\text{g L}^{-1}$, and extraction time of 22.5 min. Also, the highest absorbance (0.0968) of Cr was obtained at the pH=5, the adsorbent dosage of 0.12 g, ligand concentration of $4 \mu\text{g L}^{-1}$, and extraction time of 22.5 min.

Analysis of variance (ANOVA)

The significance and adequacy of the model were studied using ANOVA (Tables 4 and 5). The coefficients obtained from the ANOVA tables related to both ions were replaced in Eq. (2), which are described using Eqs. (4) and (5) for Cd and Cr ions, respectively.

Table 4 ANOVA for response surface quadratic model of Cd ion

Source	Sum of squares	df	Mean square	F value	P value	
Model	0.44	14	0.031	88.44	<0.0001	Significant
A—pH	0.1	1	0.10	283.73	<0.0001	
B—adsorbent dosage	3.01E-07	1	3.01E-007	8.46E-004	0.9771	
C—ligand concentration	0.019	1	0.019	54.10	<0.0001	
D—extraction time	0.12	1	0.12	324.89	<0.0001	
AB	0.020	1	0.020	55.25	<0.0001	
AC	0.037	1	0.037	103.75	<0.0001	
AD	1.39E-004	1	1.39E-004	0.39	0.5389	
BC	5.94E-003	1	5.94E-003	16.72	0.0006	
BD	8.15E-03	1	8.15E-03	22.94	0.0001	
CD	3.91E-003	1	3.91E-003	11.01	0.0036	
A ²	0.084	1	0.084	236.69	<0.0001	
B ²	7.11E-003	1	7.11E-003	19.99	0.0003	
C ²	1.84E-003	1	1.84E-003	5.19	0.0345	
D ²	0.037	1	0.037	103.51	<0.0001	
Residual	6.76E-003	19	3.56E-004	—	—	
Lack of fit	1.37E-003	10	1.37E-004	0.23	0.9845	Not significant
Pure error	5.38E-003	9	5.98E-004	—	—	
Cor total	0.45	35	—	—	—	
R ²	0.9849					
Adjusted R ²	0.9738					
Predicted R ²	0.9615					

$$\begin{aligned} \text{Abs} = & + 0.86 + 0.092A + 1.583E + 0.040C \\ & + 0.098D + 0.070AB + 0.096AC + 5.900E + 0.039BC \\ & + 0.045BD + 0.031CD + 0.10A^2 + 0.030B^2 + 0.068D^2 \end{aligned} \quad (4)$$

$$\begin{aligned} \text{Abs} = & + 0.0700 + 0.010A + 0.015B + 7.333E + 0.003C + 9.075E + 0.003D \\ & + 4.325E + 1.775E + 2.125E + 0.022BC + 4.075E + 0.003BD \\ & + 1.975E + 2.654E + 0.003A^2 + 0.012B^2 + 3.817E + 0.003C^2 + 6.854E + 0.003D^2 \end{aligned} \quad (5)$$

In addition, the probability values (p values) were used to determine the significance of the model, factors, as well as their interactions. According to the p values of Cd ion ($p < 0.05$), it could be concluded that linear coefficients except for B, interactive coefficients except for AD, and all quadratic coefficients were significant. The F value model (88.44) represented that the model was significant with a p value lower than 0.0001. Due to the p value corresponding to the lack of fit (LOF) (0.9845), this parameter is not significant, indicating that the error can be ignored and the model describes all data well. The predicted coefficient of determination (R^2) of 0.9615 has a proper agreement with the adjusted R^2 of 0.9738. Furthermore, a high value of the

R^2 equal to 0.9849 revealed a good correlation between the experimental and predicted values.

The model, all factors, their interactions (AB, BC, BD), as well as A^2 , B^2 , C^2 , and D^2 related to the Cr ion are signifi-

cant because their p value is less than 0.05. The p value of LOF is 0.9275, indicating that the model is consistent with the experimental responses owing to the larger p value than the α level (0.05). The value of R^2 is equal to 0.9858. Also, the high adjusted R^2 value (0.9754) confirms that the model is highly significant. The obtained model can well predict the experimental results because the value of the predicted R^2 is high (0.9557).

The normal plot of residuals (normal % probability versus internally studentized residuals) is illustrated in Fig. 7a and b. The normally distribution is observed for both ions because the points are satisfactorily close to the straight line and there is no variance deviation. The relationship between the variables and the response was effectually increased by this model. In addition, the high correlation between

Table 5 ANOVA for response surface quadratic model of Cr ion

Source	Sum of squares	df	Mean square	F value	p value	
Model	9.46E-003	14	6.76E-004	94.31	<0.0001	Significant
A—pH	1.23E-003	1	1.23E-003	172.19	<0.0001	
B—adsorbent dosage	2.80E-003	1	2.80E-003	390.19	<0.0001	
C—ligand concentration	6.45E-004	1	6.45E-004	90.03	<0.0001	
D—extraction time	9.88E-004	1	9.88E-004	137.87	<0.0001	
AB	7.48E-005	1	7.48E-005	10.44	0.0044	
AC	1.26E-005	1	1.26E-005	1.76	0.2006	
AD	1.81E-005	1	1.81E-005	2.52	0.1289	
BC	1.85E-003	1	1.85E-003	257.96	<0.0001	
BD	6.64E-005	1	6.64E-005	9.27	0.0067	
CD	1.56E-005	1	1.56E-005	2.18	0.1565	
A ²	5.64E-005	1	5.64E-005	7.86	0.0113	
B ²	1.21E-003	1	1.21E-003	169.31	<0.0001	
C ²	1.17E-004	1	1.17E-004	16.26	0.0007	
D ²	3.76E-004	1	3.76E-004	52.43	<0.0001	
Residual	1.36E-004	19	7.17E-006	—	—	
Lack of fit	4.02E-005	10	4.02E-006	0.38	0.9275	Not significant
Pure error	9.60E-005	9	1.07E-005	—	—	
Cor total	0.011	35	—	—	—	
R ²	0.9858					
Adjusted R ²	0.9754					
Predicted R ²	0.9557					

predicted and actual values related to the Cd and Cr ions is observed that the values are near to a straight line. The externally studentized residuals against the run number were plotted. The satisfying fit of the model can be expressed, as all the data points were obtained within the proper range (−3.74 to 3.74 for Cd and −3.68 to 3.68 for Cr).

Three-dimensional response surface plots

Figures 8 and 9 depict the three-dimensional response surface plots of both metal ions. The interaction between the parameters and determination of the optimum level related to each factor can be investigated using these figures. These kinds of plots display the effect of two variables on the response at the central point of other variables.

Figure 8a represents the interactive effect of pH and adsorbent dosage on the response surfaces (absorbance). At this step, ligand concentration and time were kept constant at 2.25 $\mu\text{g L}^{-1}$ and 22.50 min, respectively. The absorbance was enhanced with increasing pH up to 5. By increasing pH, the H^+ is diminished in the solution, leading to a decrease in the protonation effect of the COOH

group on the adsorbent surface, and the number of adsorption sites on the adsorbent surface is increased. Hence, the adsorption is improved. With a further increase of pH, the solution continuously becomes alkaline, and metal ions begin to precipitate (Rais et al. 2021). The maximum Cd absorbance of 0.9647 was obtained at 0.02 g of adsorbent dosage.

Figure 8b demonstrates the interactive effect of ligand concentration and adsorbent dosage where pH and time were kept constant at 5 and 22.5 min, respectively. With an increase in ligand concentration of 0.5 to 4 $\mu\text{g L}^{-1}$, the absorbance increased. The highest absorbance was achieved at a ligand concentration of 4 $\mu\text{g L}^{-1}$.

The effect of time and adsorbent dosage on absorbance is shown in Fig. 8c where pH and ligand concentration were kept constant at 5 and 2.25 $\mu\text{g L}^{-1}$, respectively. The Cd absorbance was found to be enhanced up to 22.5 min with an increase in adsorbent dosage from 0.02 to 0.12 g. After a contact time of 22.5 min, diminish in the remaining number of active sites on the adsorbent surface occurs.

Figure 8d reveals the effects of ligand concentration and pH when adsorbent dosage and time were kept constant at 0.07 g and 22.5 min, respectively. It was observed that

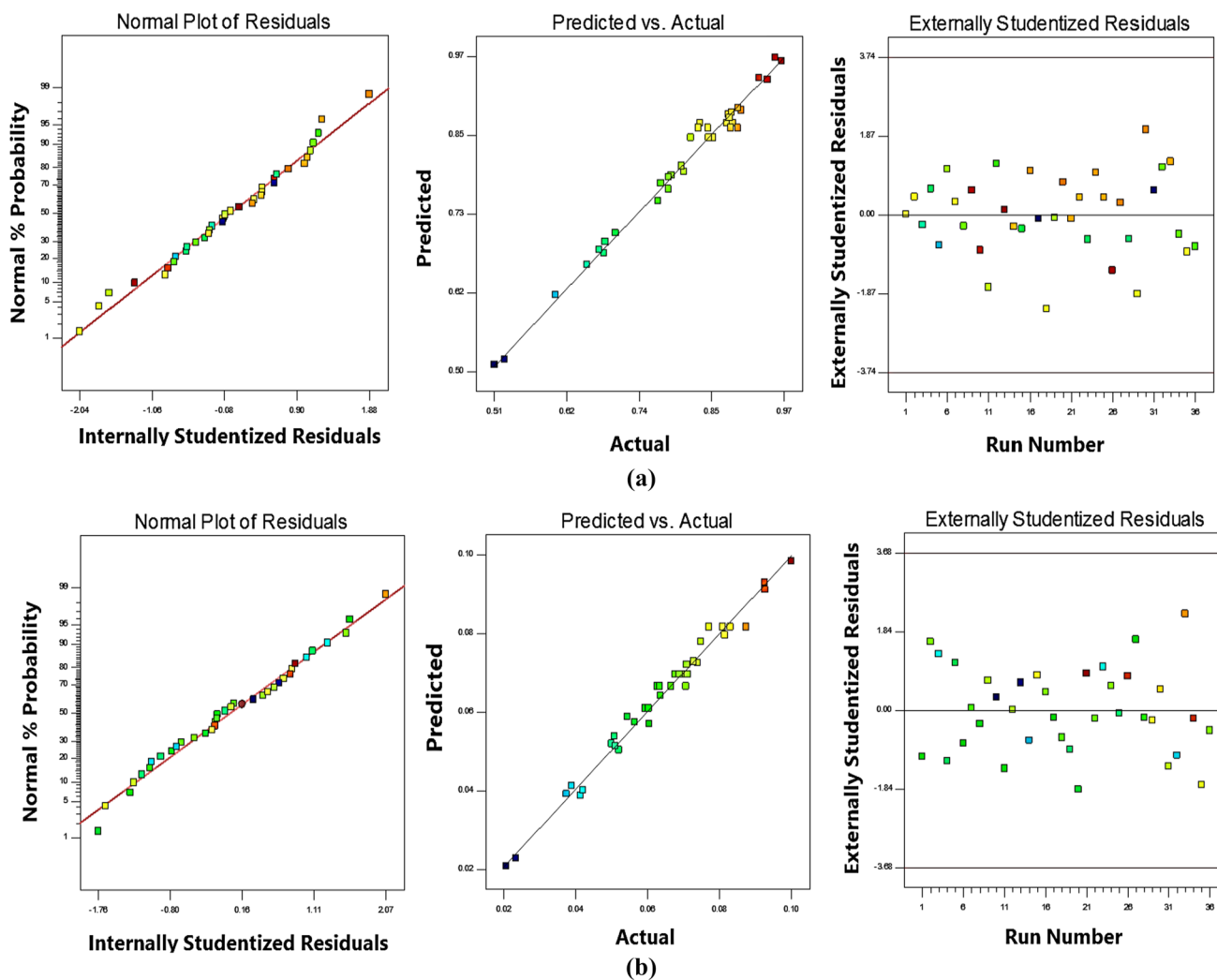


Fig. 7 Normal % probability versus internally studentized residuals, predicted versus actual values, and externally studentized residuals versus run number for **a** Cd and **b** Cr ions

with an increase in ligand concentration from 0.5 to 4, an increase in absorbance was observed. Also, when the pH was enhanced from 3 to 5, the absorbance was found to be increased.

The effect of time and ligand concentration on absorbance is depicted in Fig. 8e, where the pH and adsorbent dosage were considered 5 and 0.07 g, respectively. With an increase in the contact time from 5 to 22.5 min, the absorbance was found to be enhanced. Furthermore, an increase in ligand concentration showed an increase in response.

In the case of Cr absorbance, Fig. 9a exhibits the effects of adsorbent dosage and pH on Cr absorbance when ligand concentration and time were kept constant at $2.25 \mu\text{g L}^{-1}$ and 22.5 min, respectively. It can be seen that with an increase in adsorbent dosage from 0.02 to 0.12 g, an increase in absorbance occurs. When the pH was increased from 3 to 5, the Cr absorbance was found to be enhanced. It has already been stated that higher pH may cause metal precipitation.

Figure 9b shows the interactive effect of ligand concentration and adsorbent dosage on the absorbance of Cr where pH and time values were kept constant at 5 and 22.5 min,

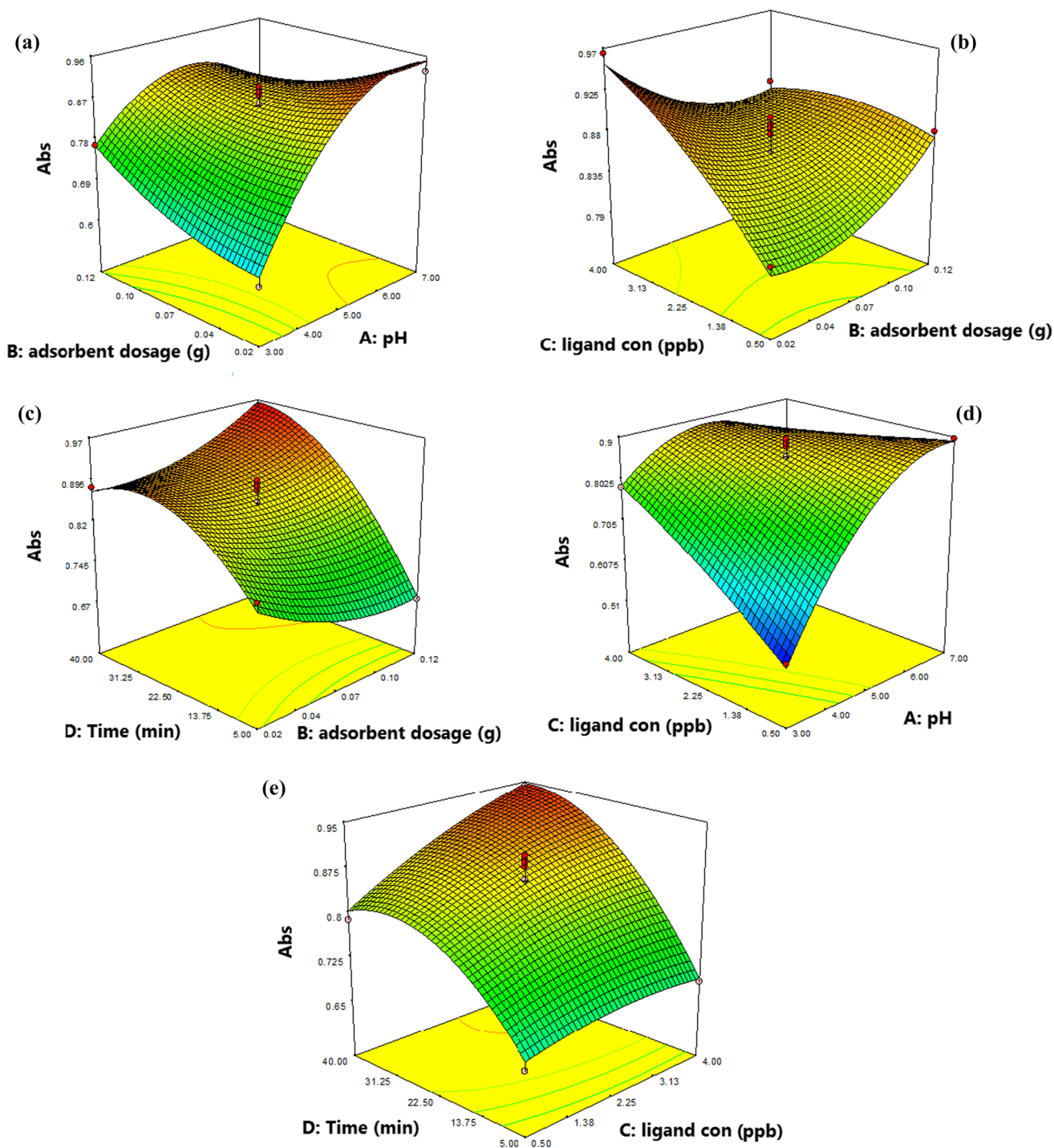


Fig. 8 3-D response surface plots of interaction effect of two independent variables: **a** adsorbent dosage and pH, **b** ligand concentration and adsorbent dosage, **c** time and adsorbent dosage, **d** ligand concentration and pH, and **e** time and ligand concentration for the absorbance of Cd ion

respectively. An increase in ligand concentration led to increase in absorbance.

By increasing contact time up to 22.5 min, as well as increasing the adsorbent dosage from 0.02 to 0.12 g the

absorbance was enhanced (Fig. 9c). By elevating the adsorbent dosage, the available active sites of the adsorbent surface were increased and more metal ions are adsorbed on the adsorbent surface.

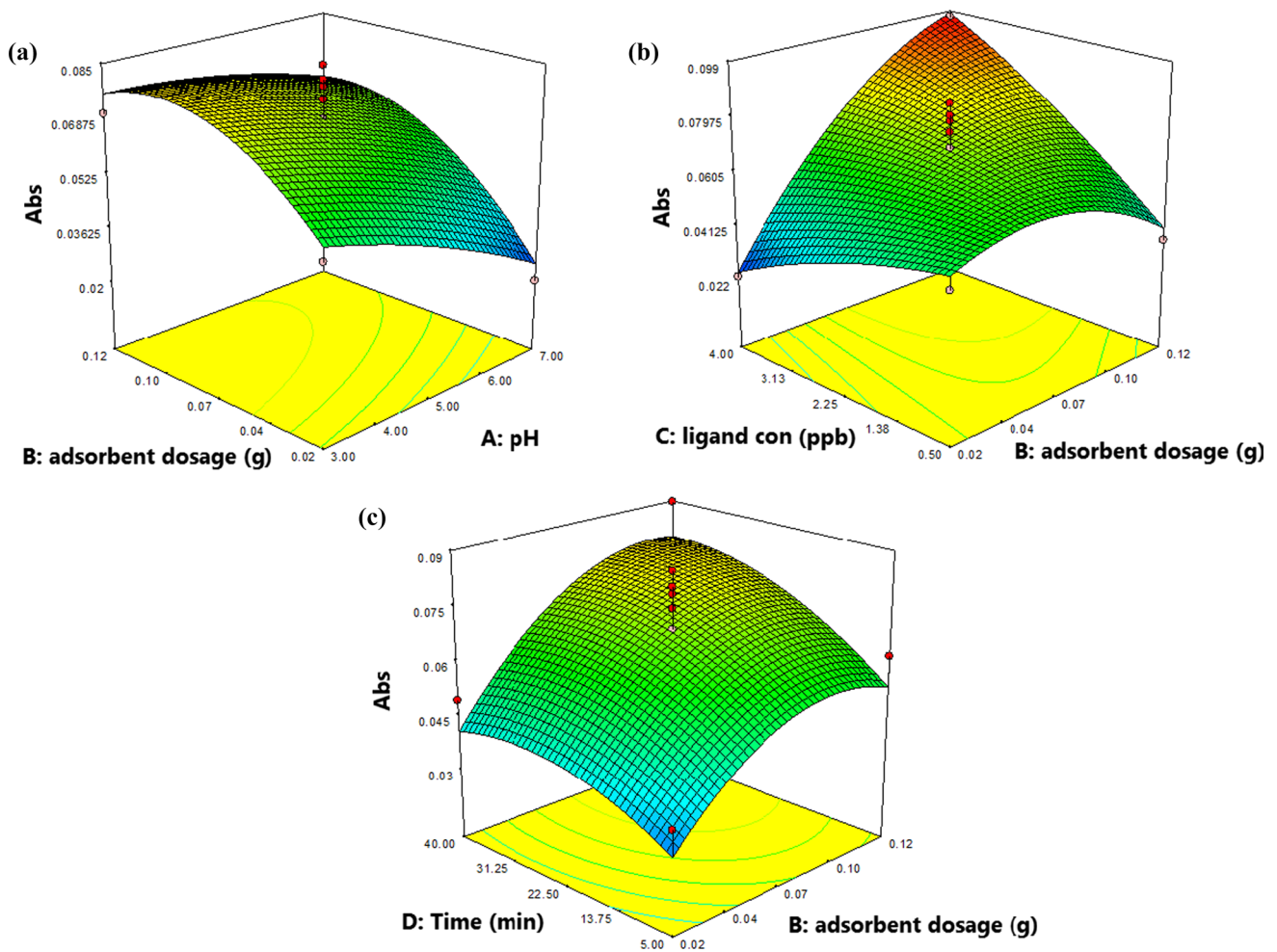


Fig. 9 3-D response surface plots of interaction effect of two independent variables: **a** adsorbent dosage and pH, **b** ligand concentration and adsorbent dosage, and **c** time and adsorbent dosage for the absorbance of Cr ion

Determination of Cd and Cr ions in real samples

The efficiency of the suggested technique for the preconcentration and extraction of the Cd, and Cr ions from real samples including basil, pennyroyal, parsley, mint, and dill was evaluated. Two various concentrations containing 10 and 20 $\mu\text{g L}^{-1}$ were used for the spike solutions. In order to determine the values of Cd and Cr ions, ETAAS method was utilized. The accuracy was represented via the recovery percentage, which calculated for each sample (Tables 6). The recovery related to the ETAAS approach was 58.63% to 99.03% and 62.86% to 89.69% for the Cd (II) and Cr (VI), respectively. In addition, the precision was studied using relative standard deviation (RSD) values, which were

found lower than 2.8% for the ETAAS, respectively. It can be concluded that the ETAAS had a significant performance. According to the results, the proposed adsorbent possesses a high potential for the effective extraction of the Cd and Cr ions from the real samples.

On the other hand, recovery percentage and RSD% related to the intra-day and inter-day were investigated with five replicate (Table 7). In the ETAAS method, this value was < 2.5 and < 2 for intra-day and inter-day, respectively. Hence, satisfactory precision was observed in this approach. Furthermore, the calculation of recovery values was accomplished and the results revealed that the recovery was higher than 97%.

Table 6 Analytical results for Cd and Cr ions in real samples with MSPE method using ETAAS ($n=5$)

Sample	Analyte	Added ($\mu\text{g L}^{-1}$)	Found ($\mu\text{g L}^{-1}$)	Recovery (%)
Basil	Cd (II)	0	5.13	–
	Cr (VI)	0	6.12	–
	Cd (II)	10.00	15.11	99.84 ± 1.36
	Cr (VI)	10.00	15.99	98.77 ± 1.75
	Cd (II)	20.00	25.2	100.38 ± 2.15
	Cr (VI)	20.00	25.9	98.98 ± 1.28
Pennyroyal	Cd (II)	0	2.66	–
	Cr (VI)	0	5.73	–
	Cd (II)	10.00	12.52	98.63 ± 1.34
	Cr (VI)	10.00	15.69	99.67 ± 1.16
	Cd (II)	20.00	22.47	99.03 ± 2.73
	Cr (VI)	20.00	25.89	100.08 ± 1.23
Dill	Cd (II)	0	8.63	–
	Cr (VI)	0	6.36	–
	Cd (II)	10.00	18.32	99.16 ± 1.54
	Cr (VI)	10.00	16.26	99.09 ± 1.56
	Cd (II)	20.00	28.15	97.66 ± 1.32
	Cr (VI)	20.00	25.67	96.58 ± 2.13

Table 7 Intra-day and inter-day accuracy (as recovery%) and precision (as RSDs%) of the methods for the real sample

Analyte	ETAAS	
	Intra-day (Recovery \pm RSD) %	Inter-day (Recovery \pm RSD) %
Cd (II)	97.80 ± 1.99	95.60 ± 1.51
Cr (VI)	93.60 ± 2.27	92.50 ± 1.03

Table 8 Tolerance limits of interfering ions in the determination of Cr(VI) and Cd(II)

Ions	Added as	Cr /mg L ⁻¹	Cd /mg L ⁻¹
Cl ⁻	NH ₄ Cl	1000	1000
F ⁻	NaF	400	300
Co ₃ ²⁻	CaCO ₃	500	500
Na ⁺	NaCl	1000	1000
Ca ²⁺	CaCl ₂	2000	2000
Fe ³⁺	Fe(NO ₃) ₃ ·9H ₂ O	1000	2000
Zn ²⁺	Zn(NO ₃) ₂	500	500
Ni ²⁺	Ni(NO ₃) ₂ ·6H ₂ O	600	500
Cu ²⁺	Cu(NO ₃) ₂ ·3H ₂ O	1000	1000
Mn ²⁺	MnCl ₂	500	500

Tolerance of other ions on the proposed method

The interference experiment was accomplished to evaluate the selectivity of the suggested approach through the determination of Cd and Cr ions along with other ions (Table 8). Therefore, different cations (Na⁺, Li⁺, Ca²⁺, Fe³⁺, Zn²⁺, Ni²⁺, Cu²⁺, Mn²⁺, Ba²⁺) and anions (Cl⁻, F⁻, Br⁻, Co³⁻) were added to the solution containing Cd(II) and Cr(VI) ions and the recovery percentage was determined for each interfering ion. The results indicated that the presence of large amounts of species in real samples had no effect on recovery of Cd and Cr ions.

Comparison with literature

The suggested approach was compared with other analytical methods described for the determination of Cd (II), Cr (VI), Cu (II), and Zn (II) in various samples in terms of LOD, LOQ, RSD, and recovery (Table 9). Compared to other extraction methods, which may have been more difficult and time-consuming to prepare the adsorbent, the proposed method is simpler and the adsorbent preparation is easier. The RSDs achieved via the present technique are satisfactory and comparable with those of the other approaches. The LOD values of both metal ions related to the ETAAS are lower than LODs of the other methods. The LOQs of the proposed technique for Cd (II) and Cr (VI) are lower than the previously reported methods. Also, the obtained recoveries were in the acceptable ranges.

LOD and LOQ are determined as $\text{LOD} = 3 \times \text{SD}/m$ and $\text{LOQ} = 10 \times \text{SD}/m$ where SD is the standard deviation of the lowest concentration in the calibration plot and m is the slope of the calibration plot (Öztürk Er et al. 2018).

Conclusion

In this study, the MSPE procedure using magnetic MWCNTs as an adsorbent was presented for the extraction and preconcentration of Cd and Cr ions from different vegetable samples prior to ETAAS detection. To optimize the magnetic extraction parameters such as pH, adsorbent dosage, ligand concentration, and extraction time, BBD was implemented. The recovery percentage and RSD values obtained from spike results proved the acceptable accuracy and precision of the technique to the selected samples. The low LODs and LOQs, as well as a good linear range related to the ETAAS

Table 9 Comparative data from studies on extraction and determination of Cd (II) and Cr (VI)

Extraction method	Detection technique	Adsorbent	Sample	Analyte	LOD ($\mu\text{g L}^{-1}$)	LOQ ($\mu\text{g L}^{-1}$)	Recovery (%)	RSD (%)	Ref
SPME ^a	FAAS	Fe ₃ O ₄ @CS ^b	Vegetable	Cd (II)	0.20	0.68	96.00	5.3	(Öztürk Er et al. 2018)
LLME ^c	FAAS	–	Vegetable	Zn (II)	0.60	–	98.40	2	(Altunay and Katin 2020)
SUPRAS-ME ^d	FAAS	–	Well water	Cd (II)	0.30	1.00	96.80	2.5	(Altunay and Katin 2020)
–	ICP-OES	AC ^e	Fruit	Cd (II)	0.17	–	100.00	3.0	(Altunay and Elik 2021)
DLLME-DES ^f	FAAS	Complexing	Milk	Cu (II)	0.38	0.80	–	3.6	(Feist and Mikula 2014)
CPE ^g	FAAS	Complexing	Aqueous	Cd (II)	0.20	–	–	2.4	(Sorouraddin et al. 2020)
MSPE ^h	FAAS	Co-Fe ₃ O ₄ NPs	Vegetable	Cd (II)	0.60	–	92.20	2.2	(Karadaş 2015)
MSPME ⁹	FAAS	Co-Fe ₂ O ₄ NPs	Oyster	Cd (II)	0.24	0.80	98.00	3.3	(Roushani et al. 2017)
MSPE	ETAAS	MWCNTs	Vegetables	Cd (II)	0.07	0.09	99.03	<2.8	(Dias et al. 2019)
				Cr (VI)	0.24	0.27	89.69	<2.2	This study

^aSolid-phase microextraction^bChitosan^cLiquid–liquid microextraction^dSupramolecular solvent microextraction^eActivated carbon^fDispersive liquid–liquid microextraction-deep eutectic solvents^gCloud point extraction^hMagnetic solid-phase extractionⁱMagnetic solid-phase microextraction

for both ions were provided. The magnetic adsorbent carrying the metal ion could be simply separated from the aqueous solution using an external magnetic field without filtration or centrifugation process. The MSPE approach is fast, simple, efficient, and inexpensive, which is convenient to complicated matrices such as vegetable samples with satisfactory recovery.

References

- Abrham F, Gholap AV (2021) Analysis of heavy metal concentration in some vegetables using atomic absorption spectroscopy. *Pollution* 7:205–216
- Abu-El-Halawa R, Zabin SA (2017) Removal efficiency of Pb, Cd, Cu and Zn from polluted water using dithiocarbamate ligands. *J Taibah Univ Sci* 11:57–65
- Altunay N, Elik A (2021) Ultrasound-assisted alkanol-based nanostructured supramolecular solvent for extraction and determination of cadmium in food and environmental samples: Experimental design methodology. *Microchem J* 164:105958
- Altunay N, Katin KP (2020) Ultrasonic-assisted supramolecular solvent liquid–liquid microextraction for determination of manganese and zinc at trace levels in vegetables: experimental and theoretical studies. *J Mol Liq* 310:113192
- Arora R (2019) Adsorption of heavy metals: a review. *Mater Today Proc* 18:4745–4750
- Arpa C, Arıdaşır I (2019) Ultrasound assisted ion pair based surfactant-enhanced liquid–liquid microextraction with solidification of floating organic drop combined with flame atomic absorption spectrometry for preconcentration and determination of nickel and cobalt ions in vegetable and herb samples. *Food Chem* 284:16–22
- Ashraf I, Ahmad F, Sharif A, Raza Altaf A, Teng H (2021) Heavy metals assessment in water, soil, vegetables and their associated health risks via consumption of vegetables District Kasur, Pakistan. *SN Appl Sci* 3:552
- Barbosa MO, Ribeiro RS, Ribeiro ARL, Pereira FR, M, Silva AMT, (2020) Solid-phase extraction cartridges with multi-walled carbon nanotubes and effect of the oxygen functionalities on the recovery efficiency of organic micropollutants. *Sci Rep* 10:22304
- Chen B, Wang S, Zhang Q, Huang Y (2012) Highly stable magnetic multiwalled carbon nanotube composites for solid-phase extraction of linear alkylbenzene sulfonates in environmental water samples prior to high-performance liquid chromatography analysis. *Analyst* 137:1232–1240
- Commission Regulation (EU) EC (2011) Amending regulation (EC) No 1881/2006 setting maximum levels for certain contaminants in foodstuffs. *Off J Eur Union* 111(2011):3–6
- Daşbaşı T, Saçmacı S, Ülgen A, Kartal S (2015) A solid phase extraction procedure for the determination of Cd(II) and Pb(II) ions in food and water samples by flame atomic absorption spectrometry. *Food Chem* 174:591–596
- de Oliveira M, Lopes A, Rocha Chellini P, Arromba de Sousa R (2020) Cadmium and chromium determination in herbal tinctures

- employing direct analysis by graphite furnace atomic absorption spectrometry (GF-AAS). *Anal Lett* 53:2096–2110
- Dias FS, Guarino ME, Costa Pereira AL, Pedra PP, Bezerra MA, Gustavo Marchetti S (2019) Optimization of magnetic solid phase microextraction with CoFe_2O_4 nanoparticles for preconcentration of cadmium in environmental samples by flame atomic absorption spectrometry. *Microchem J* 146:1095–1101
- Divrikli U, Arslan Kartal A, Soylak M, Elci L (2007) Preconcentration of Pb(II), Cr(III), Cu(II), Ni(II) and Cd(II) ions in environmental samples by membrane filtration prior to their flame atomic absorption spectrometric determinations. *J Hazard Mater* 145:459–464
- Feist B, Mikula B (2014) Preconcentration of heavy metals on activated carbon and their determination in fruits by inductively coupled plasma optical emission spectrometry. *Food Chem* 147:302–306
- Hagarov I (2020) Magnetic solid phase extraction as a promising technique for fast separation of metallic nanoparticles and their ionic species: a review of recent advances. *J Anal Methods Chem* 2020:8847565
- Ibarra IS, Rodriguez JA, Galán-Vidal CA, Cepeda A, Miranda JM (2015) Magnetic solid phase extraction applied to food analysis. *J Chem* 8:1–13
- Kamel HA, El-Galil E, Amr A, Al-Omar MA, Elsayed EA (2019) Pre-concentration based on cloud point extraction for ultra-trace monitoring of Lead (II) using flame atomic absorption spectrometry. *Appl Sci* 9:4752
- Karadaş C (2015) A novel cloud point extraction method for separation and preconcentration of cadmium and copper from natural waters and their determination by flame atomic absorption spectrometry. *Water Qual Res J* 52:178–186
- Khodadadi S, Konož E, Ezabadi A, Niazi A (2021) Magnetic solid-phase extraction using ionic liquid-modified magnetic nanoparticles for the simultaneous extraction of cadmium and lead in milk samples; evaluation of measurement uncertainty. *J Mex Chem Soc* 65:457–468
- Kumar S, Prasad Sh, Kumar Yadav K, Shrivastava M, Gupta N, Nagar Sh, Bach QV, Kamyab H, Khan ShA, Yadav S, Chand Malav L (2019) Hazardous heavy metals contamination of vegetables and food chain: Role of sustainable remediation approaches-A review. *Environ Res* 179:108792
- Ling Y, Luo F, Zhu Sh (2021) A simple and fast sample preparation method based on ionic liquid treatment for determination of Cd and Pb in dried solid agricultural products by graphite furnace atomic absorption spectrometry. *LWT-Food Sci Technol* 142:111077
- Locatelli C, Melucci D (2013) Voltammetric method for ultra-trace determination of total mercury and toxic metals in vegetables. Comparison with spectroscopy. *Cent Eur J Chem* 11:790–800
- Lü HY, Yang SH, Deng J, Zhang ZH (2016) Magnetic Fe_3O_4 Nanoparticles as New, Efficient, and Reusable Catalysts for the Synthesis of Quinoxalines in Water. *Aust J Chem* 63:1290–1296
- Lu W, Li J, Sheng Y, Zhang X, You J, Chen L (2017) One-pot synthesis of magnetic iron oxide nanoparticle-multiwalled carbon nanotube composites for enhanced removal of Cr(VI) from aqueous solution. *J Colloid Interface Sci* 505:1134–1146
- Manzoor J, Sharma M, Ahmad Wani KH (2018) Heavy metals in vegetables and their impact on the nutrient quality of vegetables: a review. *J Plant Nutr* 41:1–20
- Mohamad Nasir AN, Yahaya N, Nadhirah Mohamad Zain N, Lim V, Kamaruzaman S, Saad B, Nishiyama N, Yoshida N, Hirota Y (2019) Thiol-functionalized magnetic carbon nanotubes for magnetic micro-solid phase extraction of sulfonamide antibiotics from milks and commercial chicken meat products. *Food Chem* 276:458–466
- Mohammad Sorouraddin S, Ali Farajzadeh M, Dastoori H (2020) Development of a dispersive liquid-liquid microextraction method based on a ternary deep eutectic solvent as chelating agent and extraction solvent for preconcentration of heavy metals from milk samples. *Talanta* 208:120485
- Odobasic A, Sestan I, Bratovic A (2017) The extraction of heavy metals from vegetable samples. ingredients extraction by physico-chemical methods in food. Academic Press, pp 253–273
- Onyebuchi C, Kavaz D (2020) Effect of extraction temperature and solvent type on the bioactive potential of *Ocimum gratissimum* L. extracts. *Sci Rep*. <https://doi.org/10.1038/s41598-020-78847-5>
- Öztürk Er E, Maltepe E, Bakirdere S (2018) A novel analytical method for the determination of cadmium in sorrel and rocket plants at ultratrace levels: magnetic chitosan hydrogels based solid phase microextraction-slotted quartz tube flame atomic absorption spectrophotometry. *Microchem J* 143:393–399
- Palisoc Sh, Cedrickd Estioko L, Natividad M (2018) Voltammetric determination of lead and cadmium in vegetables by graphene paste electrode modified with activated carbon from coconut husk. *Mater Res Express* 5:085035
- Parmar P, Shukla A, Goswami D, Patel B, Saraf M (2020) Optimization of cadmium and lead biosorption onto marine *Vibrio alginolyticus* PBR1 employing a Box-Behnken design. *Chem Eng J Adv* 4:100043
- Pashai Gatabi M, Milani Moghaddam H, Ghorbani M (2016) Efficient removal of cadmium using magnetic multiwalled carbon nanotube nanoadsorbents: equilibrium, kinetic, and thermodynamic study. *J Nanopart Res* 18:189
- Polat S, Sayan P (2019) Application of response surface methodology by a Box-Behnken design for struvite precipitation. *Adv Powder Technol* 30:2396–2407
- Pozzatti MS, Borges AR, Dessuy MB, Vale MR, Welz B (2017) Determination of cadmium, chromium and copper in vegetables of the Solanaceae family using high-resolution continuum source graphite furnace atomic absorption spectrometry and direct solid sample analysis. *Anal Methods* 9:329–337
- Rais S, Islam A, Ahmad I, Kumar S, Chauhan A, Javed H (2021) Preparation of a new magnetic ion-imprinted polymer and optimization using Box-Behnken design for selective removal and determination of Cu(II) in food and wastewater samples. *Food Chem* 334:127563
- Rotimi Ipeiyeda A, Ruth Ayoade A (2017) Flame atomic absorption spectrometric determination of heavy metals in aqueous solution and surface water preceded by co-precipitation procedure with copper(II) 8-hydroxyquinoline. *Appl Water Sci* 7:4449–4459
- Roushani M, Mmohammad Baghelani Y, Abbasi Sh, Mavaei M, Zia Mohammadi S (2017) Flame atomic absorption spectrometric determination of cadmium in vegetable and water samples after preconcentration using magnetic solid-phase extraction. *Int J Veg Sci* 23:304–320
- Saçmacı S, Kartal S (2010) Determination of some trace metal ions in various samples by FAAS after separation/preconcentration by copper(II)-BPHA coprecipitation method. *Microchim Acta* 170:75–82
- Sadegh H, Shahryari-ghoshekandi R, Kazemi M (2014) Study in synthesis and characterization of carbon nanotubes decorated by magnetic iron oxide nanoparticles. *Int Nano Lett* 4:129–135
- Soni G, Jain K, Soni P, Kumari Jangir R, Vijay YK (2020) Synthesis of multiwall carbon nanotubes in presence of magnetic field using underwater arc discharge system. *MaterToday Proc* 30:225–228
- Wang Z, Xu W, Jie F, Zhao Z, Zhou K, Liu H (2021) The selective adsorption performance and mechanism of multiwall magnetic carbon nanotubes for heavy metals in wastewater. *Sci Rep* 11:16878
- Yilmaz E, Soylak M. Type of new generation separation and preconcentration methods. In *New Generation Green Solvents for Separation and Preconcentration of Organic and Inorganic Species* 2020 Jan 1 (pp. 75-148). Elsevier.

- Zhao N, Biana Y, Dong X, Gao X, Zhao L (2021) Magnetic solid-phase extraction based on multi-walled carbon nanotubes combined ferroferric oxide nanoparticles for the determination of five heavy metal ions in water samples by inductively coupled plasma mass spectrometry. *Water Sci Technol* 84:1417–1424
- Zhong WS, Ren T, Zhao LJ (2016) Determination of Pb (lead), Cd (cadmium), Cr (chromium), Cu (copper), and Ni (nickel) in

Chinese tea with high-resolution continuum source graphite furnace atomic absorption spectrometry. *J Food Drug Anal* 24:46–55

Publisher's Note Springer Nature remains neutral with regard to jurisdictional claims in published maps and institutional affiliations.